IRAQI Academic Scientific Journals

Tikrit Journal of Engineering Sciences (2020) 27 (2): 54-64.

ISSN: 1813-162X (Print) ; 2312-7589 (Online)

Tikrit Journal of Engineering Sciences

available online at: http://www.tj-es.com

TJES Tikrit Journal of Engineering Sciences

College of Engineering

Alaaraji R M, Kashmola S Y. Evaluation of Damage Index for RC Frames with Irregular Geometrical Shape Subjected to Blast Loads. *Tikrit Journal of Engineering Sciences* 2020; **27**(2): 54- 64.

Evaluation of Damage Index for RC Frames with Irregular Geometrical Shape Subjected to Blast Loads

Riyadh M. M. Alaaraji[1*]

Sofyan Y. A. Kashmola [2]

[1] Civil Department/ Engineering College/ Mosul University/ Mosul, Iraq

[2] Department of Environmental Engineering/ College of Engineering/ Mosul University/ Mosul, Iraq

***Keywords*:**

Blast Load, Plastic Hinges, Damage Index, Ductility, Reinforced Concrete.

A R T I C L E I N F O

Article history:

Received 05 Dec. 2019

Accepted 25 Aug. 2020

Available online 15 Oct. 2020

Tikrit Journal of Engineering Sciences Tikrit Journal of Engineering Sciences Tikrit Journal of Engineering Sciences Tikrit Journal of Engineering Sciences

A B S T R A C T

The present research focuses on studying the effect of architectural shape of reinforced concrete frames resulting from irregularity of geometrical shape of building frame. The reinforced concrete Frame, consisting of eight storey and three bays, was designed by the American Code ACI-14. SAP2000 (V.20) software was used for the purposes of design, analysis, of the structural response for behavior elasto-plastic under the effect of blast loading, through a number of variables, including the maximum displacement and plastic deformations at the tip of structure, number and status of plastic hinges formed, and damage index. The interaction diagram between axial force and bending moment was adopted as a yield surface to undergo the transition from elastic to plastic behavior for the columns, while the design yield moment was defined as a yield criterion for beams. The accumulated plasticity (Plastic hinge) at the ends of structural element was used to simulate the elasto-plastic behavior . Irregularity and unsymmetrical form of frame structure have a significant effect on increasing the deformations and plastic displacements in the elements more than 40% and increasing the damage index in structure more than 18%, that is calculated on the basis of dissipated energy by plastic deformations. The distance between centers of Mass (C.M.) and Stiffness (C.S.) significantly affects the response of structure, where the plastic deformations of structural elements are in the least damage zone in case of convergence between two centers, compared to other cases of heterogeneity irregularity of geometrical shape of structure that results in diverging of these centers.

© 2019 TJES, College of Engineering, Tikrit University

DOI: http://dx.doi.org/10.25130/tjes.27.2.07

تقييم دليل الضرر للهيكل الخرساني المسلح ذات الشكل الهندسي غير المنتظم والمعرض للحمل الانفجاري

رياض مؤيد مال الله الاعرجي / قسم الهندسة المدنية/ كلية الهندسة/ جامعة الموصل/ العراق

سفيان يونس احمد كشمولة / قسم الهندسة المدنية/ كلية الهندسة/ جامعة الموصل/ العراق

الخلاصة

تركزّ البحث الحالي على دراسة تأثير الشكل المعماري للهيكل الخرساني المسلح المتمثل بتغاير الشكل الهندسي لهيكل البناية. حيث تم تصميم هيكل خرساني مسلح مكون من ثمانية طوابق وثلاثة فضاءات منتظم الشكل حسب المدونة الامريكية ACI-14. استخدم برنامج SAP2000 (V.20) لأغراض التحليل والتصميم ودراسة استجابة المنشأ للسلوك (المرن - اللدن) تحت تأثير الحمل الانفجاري وذلك من خلال عدد من المتغيرات منها الازاحة الجانبية العظمى واللدنة اعلى المنشأ، وعدد المفاصل اللدنة المتكوّنة وحالتها، ودليل الضرر. مُثِل العنصر الانشائي ثنائي الابعاد بنموذج (عتبة - عمود) ذي الثلاث درجات حرية، حيث اعتُمد مخطط التداخل بين القوة المحورية والعزم كسطح للخضوع للانتقال من السلوك المرن الى السلوك اللدن بالنسبة للأعمدة بينما حُدّد عزم الخضوع التصميمي كمعيار في الاعتاب لنفس السلوك وطبقاً لمبدأ اللدونة المتجمعة (المفاصل اللدنة) نهاية كل عنصر. اعتُبر للهيكل الخرساني غير المنتظم والمتناظر انشائياً تأثير واضح على زيادة التشوهات والازاحة اللدنة للمنشأ بأكثر من 40% وزيادة دليل الضرر المقاس بالنسبة للطاقة المتبددة بعد استجابة المنشأ بأكثر من 18%. وفق هذه الدراسة فان المسافة بين مركزي الكتلة والصلابة تؤثر بشكل كبير على استجابة المنشأ، فاذا قلّت هذه المسافة بين المركزين كانت استجابة المنشأ باقل نسبة ضرر للعناصر الانشائية مقارنة بالهياكل المختلفة في الشكل الهندسي العام من حيث تغاير المسقط الافقي للمنشأ.

الكلمات الدالة: الحمل الانفجاري، المفاصل اللدنة، دليل الضرر، المطيلية ، الخرسانة المسلحة.

[1] *Corresponding author: E-mail* : alriyadh81@yahoo.com

1. INTRODUCTION

Scientific and technological progress led to the development of methods of analysis and design of structures and the steps of analysis became simple and save a lot of time to express the (elasto - plastic) behavior in the structures better. With the increase of military actions and explosions striking in some cities of the world a new trend emerged in science of structural engineering which is the analysis and design of engineering installations prone to unexpected disasters such as explosions. In our country (Iraq), many cities and vital public and private structures were severely damaged, some of which were completely destroyed and some were partly damaged. Therefore, it is necessary to conduct a technical, structural and economic evaluation of these structures, to take the decision and the optimal procedure in terms of assessing damage to the restoration, rehabilitation or removal of the structure, in order to continue to invest these structures safely and economically [1]. Ayad B Bahnam [2] in 2010 studied the arrangement of diagonal tendon in structure on the response of reinforced concrete frames under the impact of blast loads, where he designed a three-storey concrete frame using non-linear (elasto-plastic) analysis of the structure by MATLAB program. The researcher concluded the ideal state of the arrangement of the tendon, which leads to reduce the maximum displacement and deflections and does not increase the maximum shear force in the structure by the explosion load. S.Mahdi S. Kolbadi et al. [3] Presented in 2017 a theoretical study on the evaluation of non-linear behavior of reinforced concrete structures exposed to explosive load. The researchers used two models, one with a percentage of carbon fiber and one without them. They concluded that there was an improvement in the response of the carbon fiber structure with minimal damage, with internal stress reduced by 43% and lateral displacement reduced to 30%. Mostafa A. Ismail [4] in 2017 studied the response of four-storey reinforced concrete space frame with composite column and subjected to blast load, as the structure is designed only for static loads, The researcher concluded that the use of a steel tube filled with concrete in the outer columns improves the structure response to the explosive load. Azadeh Parvin and others [5] in 2017 studied the case of collapse of concrete structures reinforced and subjected to severe blast load, where the researchers used finite element in the static and dynamic non-linear analysis for a number of scenarios of blast load, the structures was evaluated through the number of plastic hinges and its status, they concluded that the regular structures in terms of shape, rectangular and square sections of columns subject to blast load have the best response and the least damage. Sourish Mukherjee et al [6] in 2017 studied the structures resistant to blast loads, and stressed the hypothesis of the deletion of columns caused by the intensity of the explosion, and distribution of internal forces of missing columns on other internal columns at the structure. In 2018 Yehya Temsah et al. [7] studied numerical analysis of a reinforced concrete beam under the influence of blast load. The researchers used ABAQUS program for analysis with number of models to test under the effect of blast load. The researchers concluded that the stress rate has an obvious effect on the response of structure. Liu Y et al [8] in 2018 made a theoretical and practical study on the performance of reinforced concrete beams under the effect of blast load for variable distances and explosive charge. The results of the practical experiment showed that the location of the explosive charge has a large impact on the rate of damage and plastic deformations in it. Ibrahim YE et al. [9] Conducted in 2019 a study on reinforced concrete structures in two systems, the first being the external columns of reinforced concrete and the second is the same columns of the type of composite columns, The researchers compared the two models and concluded that the composite columns model, responds better to the blast load and less damage. In 2019, Asim Abbas et al. [10] conducted an experimental study on the behavior polystyrene foam of reinforced concrete sheet (RCSPs) prone to blast load, The researchers used four models of these panels to test. it has also been found that RCSP panels have a large capacity to absorb and dissipate the energy generated by the explosion. In 2019, Maria Chiquito et al. [11] studied the response of brick masonry walls under blast load. The researchers used three models of brick masonry (free fiber, glass, and carbon fiber). The researchers concluded that the percentage of damage in the construction units reinforced with carbon fiber and fiberglass is less harmful of non-reinforcement units.

The present study focuses on the evaluation of the damage index of the reinforced concrete structure having variable plan (irregular frames) that affects the center of mass and stiffness of the structure convergence or divergence of these centers directly affect the response of reinforced concrete structures subjected to blast loads. The research involved the design of a reinforced concrete structure according to the ACI-14 code [12] using SAP2000 (v.20) software [13]. The frame structure is analyzed for elasto-plastic behavior using Newmark's (predictor-corrector) approach for dynamic response.

The irregularity of geometrical shape of present building frame has been changed into different cases and redesigned with the same characteristics of reference case. Comparison of inelastic response between proposed cases of structure, exposed to the blast loading, through the lateral displacements, plastic hinges and damage index is performed.

1. Blast Loads at Surface

This type of load occurs directly on surface of the earth and is called a surface explosion. Explosion waves that reach the structure are reflective waves whose value depends on the geology and nature of the earth, as shown in Fig. 1 [14].

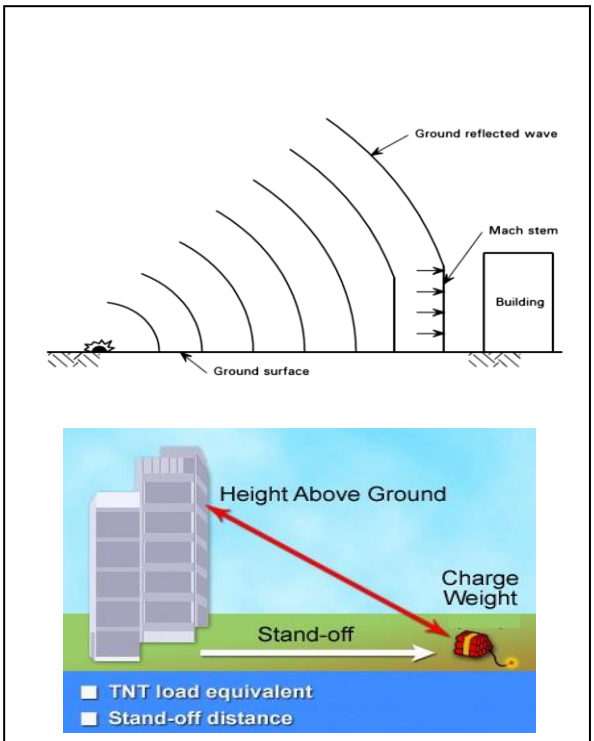

Fig.1 Surface explosion formula [14].

The scaling law is an important value for the calculation of blast load on structure. According to (Hopkinson-Cranz) law, the stand-off distance (Z) depends on the distance between source of the explosion and structure (R) and the mass of the explosion charge (W), it can be expressed by the following equation [14]:

$$Z = \frac{R}{\sqrt[3]{W}} \quad (1)$$

There is a set of logarithmic curves, based on the stand-off distance in case of surface explosions, these curves were drawn for a stand-off distance (Z) ranging from (40-0.05 m / $kg^{1/3}$) to TNT. These curves were used to calculate the blast loads applied on the structure in the present study [15].

3. Methodology of Analysis

The analysis is carried out for the following tasks, (a) Constructing the stiffness and mass matrices of structural members, (b) Calculating the force vector that is applied on the system in the current time step, and (c) Solving equations of motion by Newmark's procedure used for the nonlinear dynamic analysis. During the iterations, be sure to obtain the requested accuracy then move to a new time step, as shown in Fig. 2. Plastic displacement ,Maximum tip displacement and damage index of the structure are the results obtained at the end of analysis.

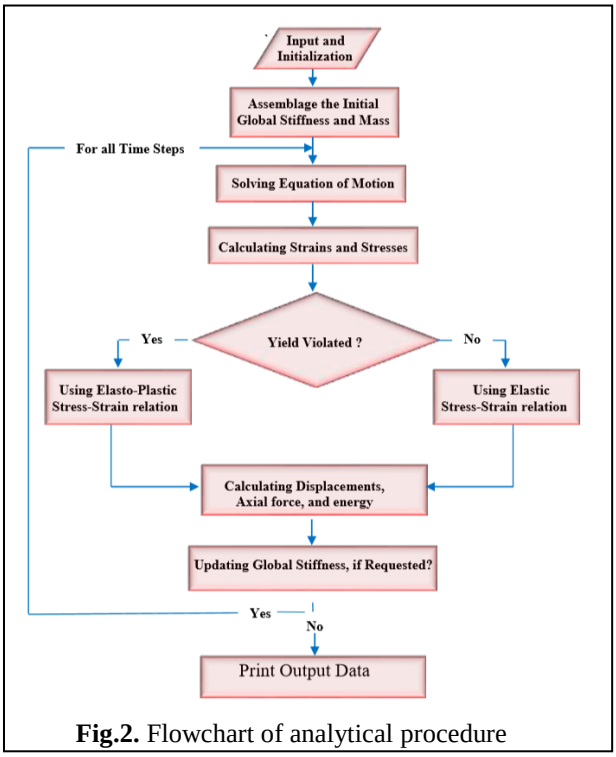

Fig.2. Flowchart of analytical procedure

4. Analytical and Mathematical Modeling

The beam-column element shown in Fig.(3-a) was used to represent the structural elements, which has plastic hinges at both ends to simulate the inelastic behavior. The elastic behavior extends along the element, whereas the (elasto - plastic) behavior is confined at both ends of the element [16]. Fig.(3-b).shows the mathematical model of the structural elements used in the present study installed forces and transitions on each element [16].

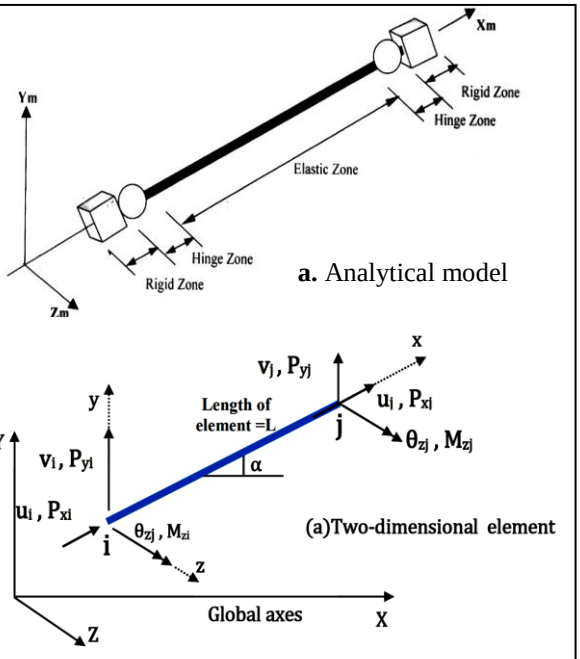

Fig.3 Analytical and mathematical model of the structural element [16]

5. Reinforced Concrete Material

The Mander (stress–strain) scheme[17] was adopted for unconfined behavior of concrete, while the Park (strain - stress) scheme [13], was adopted to govern the (elasto - plastic) behavior for reinforcing bar as shown in Fig.4. These schemes were used for calculating the yield surfaces of columns and beams.

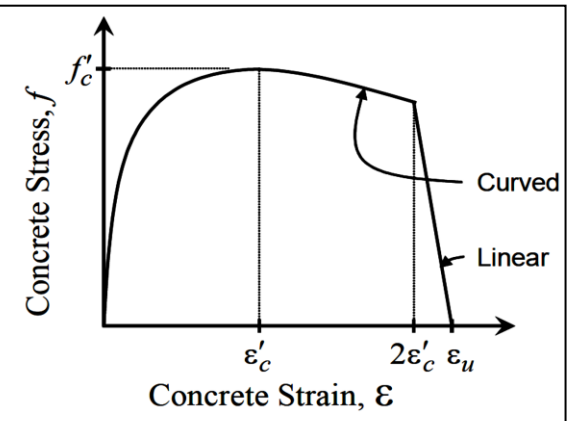

a. Stress-strain curve of unconfined concrete

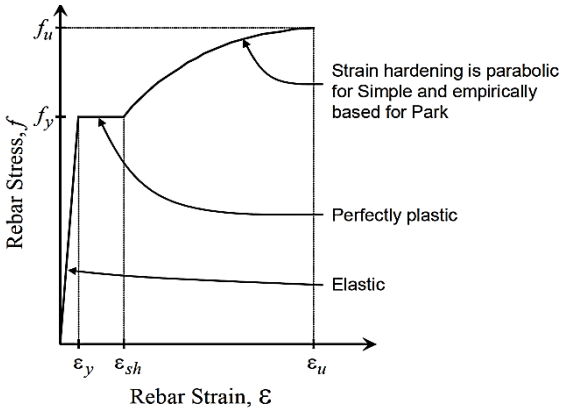

b. Stress-stress curve of reinforcing bar

Fig.4. Stress - strain curves of concrete and reinforcing bar [13].

5.1. Mathematical Relation of Concrete

The stress-strain relation suggested by Mander [17], coded in SAP2000 software, has been chosen to stimulate the unconfined behavior of concrete. When $\varepsilon \leq 2\varepsilon_c^{'}$, the governed equations are:

$$f = \frac{f'_c \times x \times r}{r-1+x^r} \quad (2)$$

$$x = \frac{\varepsilon}{\varepsilon'_c} \quad (3)$$

$$r = \frac{E}{E-\frac{f'_c}{\varepsilon'_c}} \quad (4)$$

for linear part of the curve, $2\varepsilon'_c < \varepsilon \leq \varepsilon_u$, the relation becomes:

$$f = \left(\frac{2f'_c \times r}{r-1+2^r}\right) \times \left(\frac{\varepsilon_u - \varepsilon}{\varepsilon_u - 2\varepsilon'_c}\right) \quad (5)$$

5.2. Mathematical Relation of Reinforcing Bar

Three regions govern the behavior of reinforcing steel. They are an elastic region, perfectly plastic region, and a strain hardening region. Different equations are used to define the stress-strain curve in each region, by the following equations[13]:

for $\varepsilon \leq \varepsilon_y$ (elastic region)

$$f = E\,\varepsilon \quad (6)$$

for $\varepsilon_y < \varepsilon \leq \varepsilon_{sh}$ (perfectly plastic region)

$$f = f_y \quad (7)$$

for $\varepsilon_{sh} < \varepsilon \leq \varepsilon_u$ (Park region)

$$f = f_y \left(\frac{m(\varepsilon-\varepsilon_{sh})+2}{60(\varepsilon-\varepsilon_{sh})+2} + \frac{(\varepsilon-\varepsilon_{sh})(60-m)}{2(30r+1)^2}\right) \quad (8)$$

$$r = \varepsilon_u - \varepsilon_{sh} \quad (9)$$

$$m = \frac{\left(\frac{f_u}{f_y}\right)(30\,r+1)^2 - 60\,r - 1}{15\,r^2} \quad (10)$$

Consideration has been given to reduce the stiffness of structural elements (columns and beams) according to FEMA-3٥٦ code, as shown in Table 1. It is worth noting that the structural elements are designed with the ultimate strength method [18].

Table 1 Reduction values of flexural stiffness for columns and beams [19].

Component	Effective Stiffness Values		
	Flexural rigidity	Shear Rigidity	Axial Rigidity
Nonprestress Beam	$0.5E_cI_g$	$0.4E_cA_w$	-
Column with compression due to design gravity load≥ $0.5A_gf'_c$	$0.7E_cI_g$	$0.4E_cA_w$	E_cA_g

6. Behavior of Plastic Hinges

The behavior of plastic hinge after formation in the member depends on the relation of moment-rotation (M-θ) of that member shown in Fig.5. There are special Tables in ATC-40 and FEMA-3٥٦ codes which determine the values of rotations during elastic and plastic stages, depending on the structural properties which include section dimensions, reinforcing ratio and other analytical values [19].

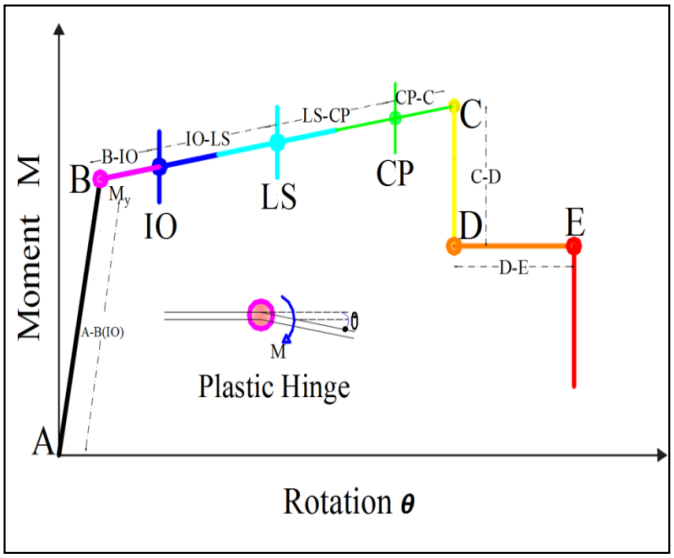

6.1. Performance Levels

Three points labeled *IO*, *LS* and *CP* shown in Fig.5 are used to define the Acceptance Criteria or performance level for the plastic hinge formed near the joints (at the ends of beams and columns). *IO*, *LS* and *CP* stand for ***I**mmediate **O**ccupancy*, ***L**ife **S**afety* and ***C**ollapse **P**revention*, respectively. The values assigned to each of these points vary depending on the type of member as well as many other parameters defined in the ATC-40 and FEMA-356 documents. Table 2. describes the structural performance levels of the concrete frames, through plastic hinges formed in the structural elements[19].

Table 2. Description of performance levels of the concrete frame[19].

Element	Type	Structural Performance Levels		
		Collapse Prevention (CP)	Live Safety (LS)	Immediate Occupancy (IO)
Concrete	Primary	Extensive cracking and hinge formation in ductile elements. Limited cracking and/or splice failure in some nonductile columns. Severe damage in short columns.	Extensive damage to beam. Spalling of cover and shear cracking (<1/8" width)for ductile columns. Minor spalling in nonductile columns. joint cracks <1/8" wide.	Minor hairline cracking. Limited yielding possible at a few locations .No crushing (strain below 0.003).
	Secondary	Extensive spalling in columns (limited shortening) and beam severe joint damage. Some reinforced buckled.	Extensive cracking and hinge formation in ductile elements. Limited cracking and/or splice failure in some nonductile columns. Severe damage in short columns.	Minor spalling in a few places in ductile columns and beams. Flexural cracking in beams and columns. Shear cracking in joints <1/16" width

6.2. Yield Surface of the Frame Members

The interaction diagram between the ultimate axial force p_u and bending moment m_u, is adopted to model the yield surface for two dimensional analysis of the reinforced concrete columns.

The development of axial force-bending moment interaction curve for columns is performed by SAP2000 software according to ACI code procedure, that requires (i) stress-strain relations for plain concrete and reinforcing steel previously shown in Fig.4. and (ii) dimensions of the section and the amount and locations of reinforcement [16]. For beams, the yield moment, calculated according to ACI code, is to be the yield criteria to transition from the elastic to plastic behavior during the analysis.

6.2.1. Inelastic Analysis of Reinforced Concrete

In general, the yield condition of the frame members can be expressed as [16]:

$$f^* = f(p_k) = 1.0 \quad (11)$$

where p_k represents the nodal forces or stress resultants; f <1 implies an elastic state; f =1.0 represents yielding and f >1.0 represents non admissible state. In classical theory of plasticity, the flow rule states that the plastic deformation rates are linearly related to their corresponding force (or stress) rates [16]. The associated flow rule can be written as:

$$\{du_p\} = \lambda . \{g\} \quad (12)$$

in which $\{du_p\}$ is plastic components of the incremental nodal displacements, λ is flow constant, and $\{g\}$ is gradient of the yield surface.

In the elastic-perfectly plastic material, there is no secondary plastic work. This implies that the increment of the nodal forces dp corresponding to a plastic deformation of a particular cross-section must be tangent to the yield surface.

$$du_p^T . dp = 0 \quad (13)$$

by using the above equations, the flow constant can be derived when the incremental nodal displacement of the element is decomposed into elastic and plastic components.

$$du = du_e + du_p \quad (14)$$

The elastic components of displacements will create incremental nodal forces dp:

$$dp = k_e . du_e \quad (15)$$

or $$dp = k_e . (du - du_p) \quad (16)$$

where k_e is the elastic stiffness matrix of the element.

substituting by the value of du_p from Eq. (18), the resulting equation is:

$$dp = k_e . du - k_e . g . \lambda \quad (17)$$

Multiplying the two sides of Eq(19) by g^T and using the flow rule and normality condition referred in Eq(18) and Eq (19) respectively, this yield:

$$g^T . dp = g^T . k_e . du - g^T . k_e . g . \lambda = 0 \quad (18)$$

solving for λ, will gives:

$$\{\lambda\} = [g^T . k_e . g]^{-1} g^T . k_e . du \quad (19)$$

$\lambda \geq 0$ implies loading condition, and $\lambda < 0$ implies elastic unloading condition.

7. Numerical Application

The reinforced concrete frame shown in Fig.6 is designed according to ACI-14 code [12], whereas the properties of concrete sections, details of static loads, as well as the blast load are shown in Table 3. Dynamic characteristics of structure are 5% damping ratio, and (0.002) time step size Newmark's (predicted – corrected) approach was used to perform the nonlinear dynamic analysis of structure [20].

The structure was subjected to an explosive charge of (15 Ton) TNT at a distance of (19 m) from the building, where the equivalent triangular blast load was calculated at the middle of building height and was equally applied at nodes opposite of explosion. Fig.7 shows the proposed cases of geometrical shapes verses to reference case (A).

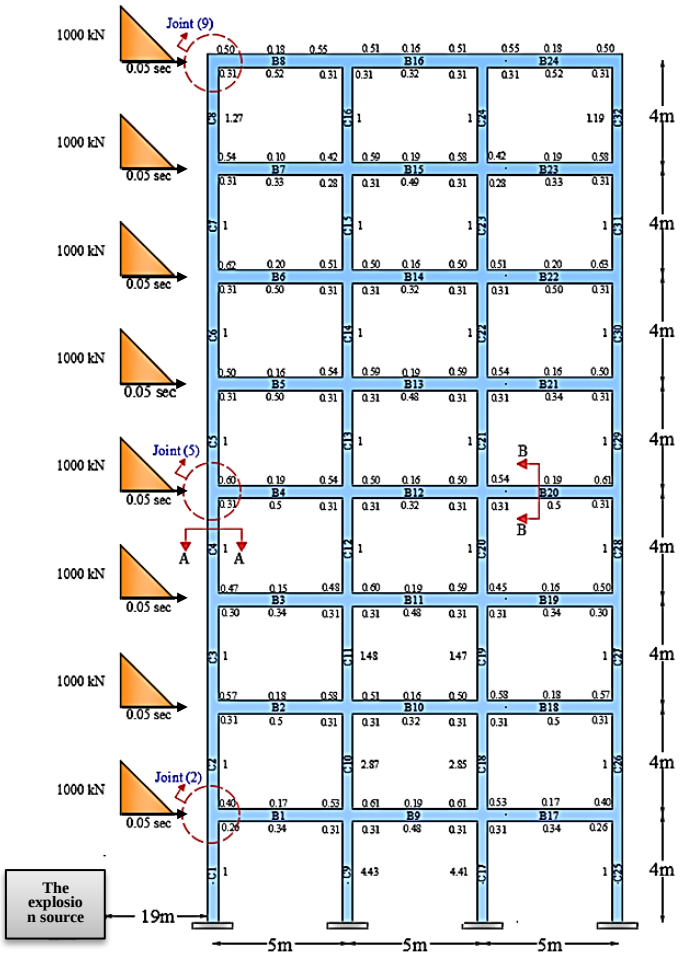

Fig.6 Details of reinforced concrete frame with reinforcement ratio, case (A)

(19)

Table 3 Structure properties (cases A,H,I)

Properties				Numerical value
Compressive strength of concrete f_c'				25.0 MPa
Elastic modulus of concrete				23650 MPa
Density of concrete				2350 kg/m^3
Yield stress of reinforcing bar f_y				414.0 MPa
Dead load				30.0 kN/m.
Live load				10.0 kN/m
Blast load				1000 kN
Time period of blast load				0.05 sec
Yield surface for columns				P-M_3
Yield surface for beams				M_3
Column	h	400mm	Beam	500mm
	b	400mm		300mm

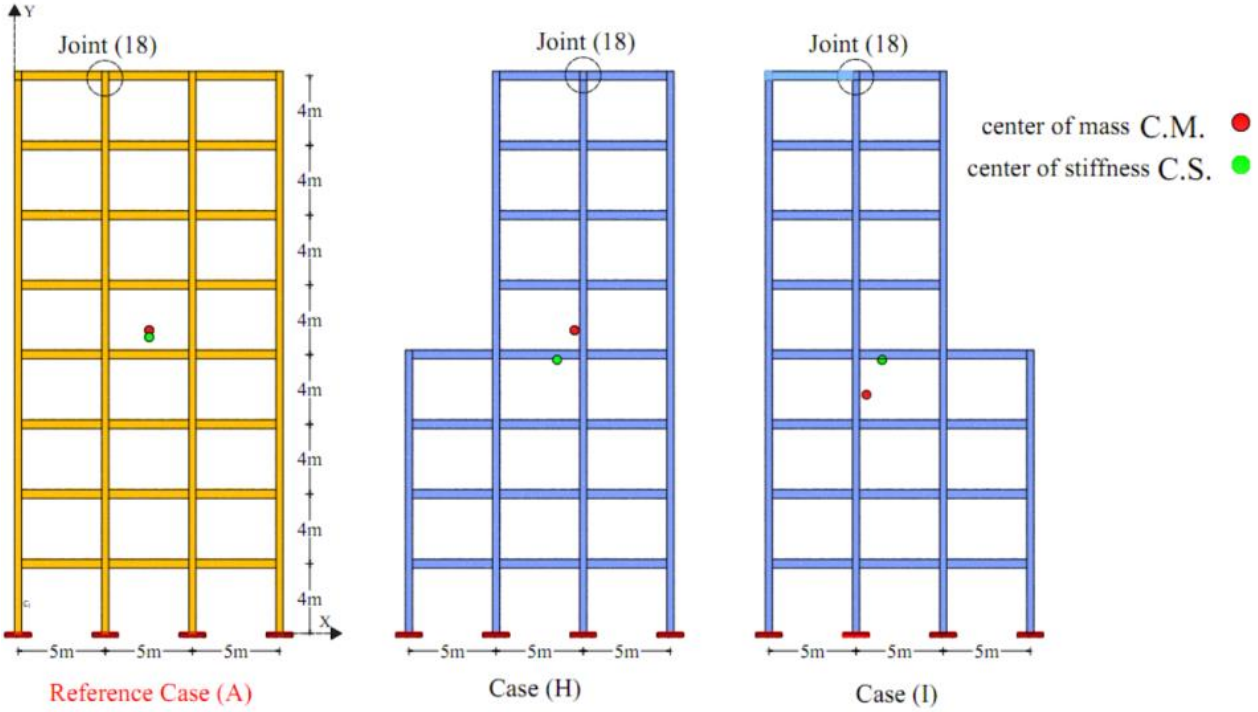

Fig.7 The proposed cases of geometrical shape *vs.* reference case (A)

7.1. Maximum and Residual Plastic Displacements:

The results, shown in Figs.8 and 9, of the nonlinear dynamic analysis of structure, exposed to blast load, gave a congruence in the cases of H and I with increase of maximum displacement by 40%, and residual plastic displacement by 56% compared to the reference case A. That increasing is due to deletion of a number of structural elements as a result of architectural design.

Removing parts of the upper stories of structure usually leads to spacing in centers of mass and stiffness and therefore additional moments and forces result in increasing of plastic deformation and damage index in the structural elements.

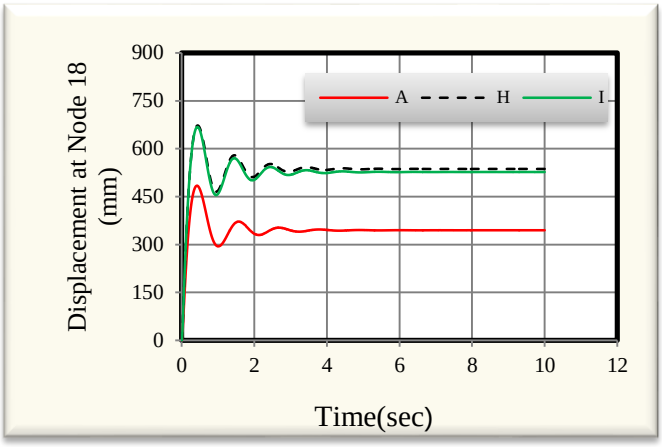

Fig.8 Lateral displacement with time at node (18) for cases of A, H, I

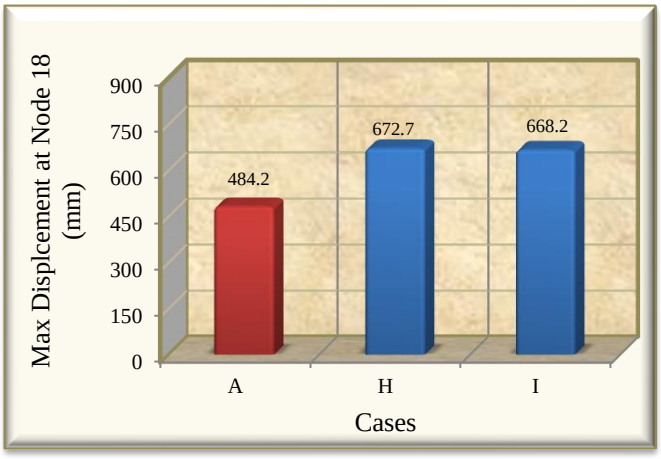

Fig. 9 Maximum lateral displacement at node (18) for cases of A, H and I

The knowledge of stiffness center has a role in engineering stability of the structure. The architectural design is preferable that the building block be as uniform and symmetrical as possible. The convergence between centers of mass and stiffness is of great importance in reducing the damage of structure and its plastic deformations. Table 4 shows the difference between two centers and gives total number of plastic hinges formed in the elements of structure within damage region(C-D).

7.2. Plastic Hinges:

Irregularity as well as reduced stiffness of structure in cases of H and I led to increasing The number of plastic hinges in the elements compared to the reference regular case (A) as shown in Fig.10. It is worth noting that the ATC-40 and FEMA-356 codes explain the damage classification in the elements depending on the amount of plastic rotation (plastic deformation), which occurs in these elements, and also show the percent of damage through the color change of plastic hinges shown in Fig.1

Table 4. Number of plastic hinges in the most damage region (C-D)

Cases	The difference between centers of mass and stiffness in X- direction (cm)	The difference between centers of mass and stiffness in Y- direction (cm)	Number of plastic hinges within (C-D) region according to FEMA classification
A	٠	35	15
I	90	200	39
H	123	170	٢٩

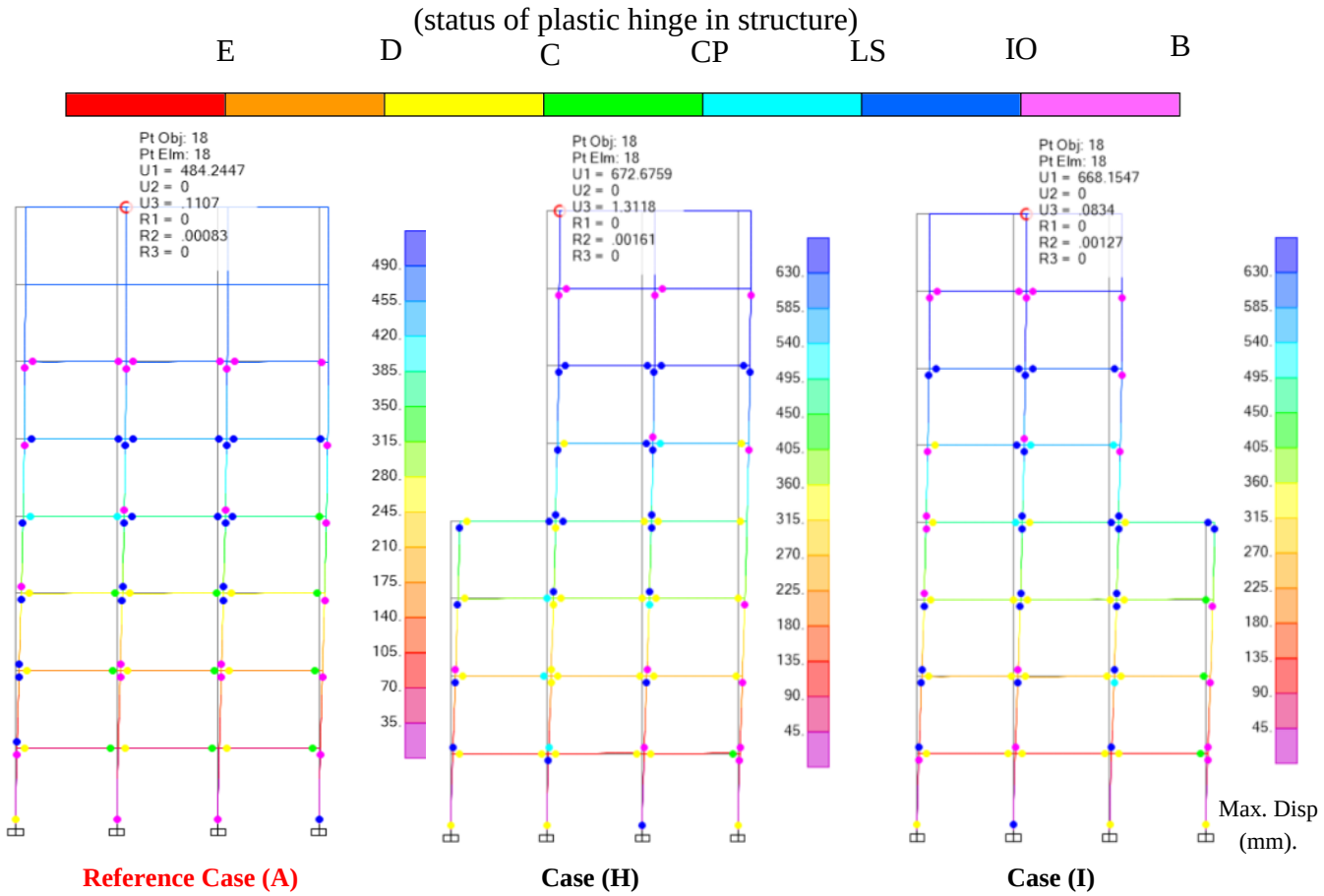

Fig. 10 status of plastic hinges and maximum displacement at node (18) of cases A, H, I

7.3.Damage and Ductile Indices:

To evaluate the reinforced concrete structures damage and ductility for empirical equations for previous researches are used [21,22].

$$DI_{Eg.} = \frac{E_h}{2\times E_p + E_h} * 100 \quad (20)$$

$$DI_{disp.} = \frac{U_{residual}}{U_{max.}} * 100 \quad (21)$$

$$\mu = \frac{U_{max}}{U_{yield}} \quad (22)$$

The damage and ductility indices of structure was calculated as in Table 5.The Figs. 11 and 12 show the relationship of damage index with the number and status of the plastic hinges in beams and columns. Increasing the damage index for cases H and I, compared to case A, by 18% and 20%, respectively, due to removing parts of the structure which results in reduction of overall stiffness of elements, and formation of more plastic hinges within the damage limits (C-D) as shown in the Figs.11 and 12, this usually have a significant impact on increasing the damage rate of structure. The ductility index (μ) shown in Table 5 reflects the opposite behavior of damage index .

Table 5. Damage and ductile indices

Cases	$\left(\frac{E_k}{E_I}\right)$ %	$\left(\frac{E_p}{E_I}\right)$ %	$\left(\frac{E_h}{E_I}\right)$ %	Damage Index $DI_{Eg.}$ %	Damage Index $DI_{disp.}$ %	Ductility Index μ
A	80.6	9.8	32.0	62	71	14
I	83.4	7.2	40.0	73	79	23
H	83.4	7.0	39.3	74	80	24

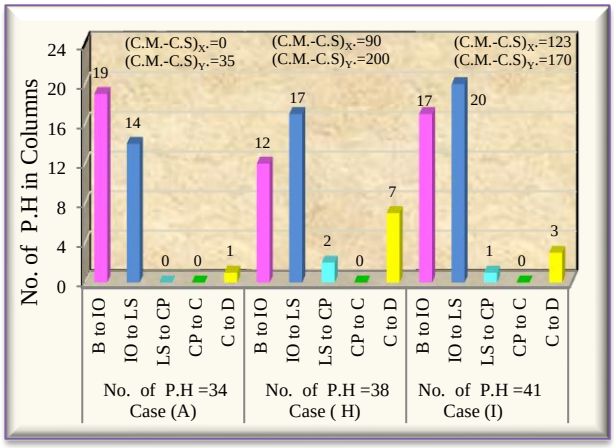

Fig. 11 Plastic hinges and its status in columns for cases A, H, and I

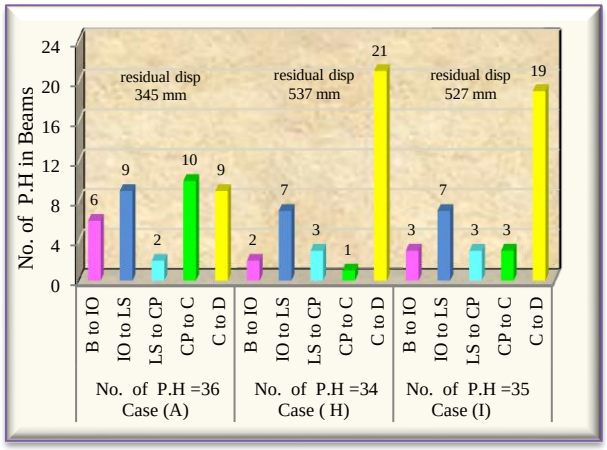

Fig. 12 Plastic hinges and its status in beams for cases A, H, and I

8. Conclusions

The results obtained showed that the symmetrical and regular state of structure leads to convergence between the centers of mass and stiffness compared with other irregular cases. The structural response to dynamic blast loads is to be in the following conclusions:

- The residual plastic displacement at the end of elasto-plastic analysis in case of irregular frames exceeded the regular reference state by 56%.
- The ratio of dissipated to input energies in case of irregular frames increased by 25% compared to the regular reference case, while the ductility increased by 71%.
- Increasing the damage index for irregular cases compared reference one by 18% and 20%, respectively, because of the divergence between centers of mass and stiffness of the structure.
- Reduced stiffness due to removing parts of the structure resulted in large deformations in the structural elements by 40 % increasing.
- The number of plastic hinges formed within the limits of large damage (C-D) are concentrated in the columns and beams in the first stories for irregular case, this usually have a significant impact on increasing the damage rate of structure.

9. References

[1] Hait Pritam, Arjun Sil, Satyabrata Choudhury. Overview of Damage Assessment of Structures. *Current Science* 2019**; 1**(117) 64.

[2] Bahnam, AB. Tendons Arrangement Effects on Reinforced Concrete FramesUnder Blast Loading. *Tikrit Journal of Engineering Sciences* 2010;**17** (3): 22-30.

[3] Kolbadi, Seyed MS, Heydar D, S. Mohammad S. Evaluation of Nonlinear Behavior of Reinforced Concrete Frames by Explosive Dynamic Loading Using Finite Element Method. *Civil Engineering Journal* 2018;**3** (12): 1198- 1207.

[4] Ismail M, Ibrahim Y, Marwa N, Mohamed M Ismail. Response of A 3D Reinforced Concrete Structure to Blast Loading. *Int. J. Adv. Appl. Sci* 2017;**4** (10): 46-53.

[5] Parvin A, Omid K, David C, Janet R. Collapse Analysis Concrete Frame Structures Subjected to Extreme Loading. Conference Paper 2017 September.

[6] Mukherjee S, Rittik B, Aparna D, Sulagno B. Review Paper on Blast Loading and Blast Resistant Structures. *International Journal of Civil Engineering and Technology (IJCIET)* 2017 August; **8**(8): 988–996.

[7] Temsah Y, Ali J, Jamal K, M. Sonebi. Numerical analysis of a reinforced concrete beam under blast loading. In MATEC Web of Conferences 2018, vol. 149, p. 02063. EDP Sciences,.

[8] Liu, Yan, Jun-bo Yan, Feng-lei Huang. Behavior of reinforced concrete beams and columns subjected to blast loading. *Defence Technology* 2018;**14** (5): 550-559.

[9] Ibrahim YE, Mostafa AI, Marwa N. Response of Reinforced Concrete Frame Structures under Blast Loading. *Procedia engineering* 2017; (171): 890-898.

[10] Abbas A, Mohammad A, Naveed A, Izaz A. Behavior of Reinforced Concrete Sandwiched Panels (RCSPs) under Blast Load. *Engineering Structures* 2019;181:476-490.

[11] Chiquito, M., L. M. López, R. Castedo, A. Pérez-Caldentey, and A. P. Santos. "Behaviour of Retrofitted Masonry Walls Subjected to Blast Loading: Damage assessment." *Engineering Structures* 2019;201: 109805.

[12] American Concrete Institute. Building Code Requirements for Structural Concrete (ACI 318 -14. American Concrete Institute. ACI, 2014.

[13] CSI (Computers and Structures, Inc.). CSI Analysis Reference Manual for SAP2000, ETABS, SAFE, and CSi Bridge. (2011).

[14] United States. Department of the Army. *Structures to Resist The Effects of Accidental Explosions*. 1991;**88**(22): Departments of the Army, Navy, and Air Force,

[15] Karlos V, George S. Calculation of Blast Loads for Application to Structural Components. Luxembourg: Publications Office of the European Union (2013).

[16] Kashmola SY, Nonlinear Dynamic Analysis of Soil-Frame Interaction Problems Ph.D.Thesis. Mosul University Mosul , Iraq, 2007, pp.116

[17] Mander JB, Priestley MJN, Park R.. Theoretical Stress-Strain Model for Confined Concrete. *Journal of Structural Engineering. ASCE* 1984. **114**(3): 1804-1826.

[18] ASCE. Prestandard and Commentary for The Seismic Rehabilitation of Buildings (FEMA 356). Prepared for FEMA (2000).

[19] Comartin C R. Niewiarowski, Rojahn C. ATC-40 Seismic evaluation and retrofit of Concrete Buildings. SSC 96 1 (1996).

[20] Clough RW, Penzien J. Dynamics of Structures, 3rd ed, University of California Berkeley, Computers and Structures, Inc., USA, 2003,pp.234-245.

[21] Cao VV, Hamid RR, Mahmud A, Hassan B. A New Damage Index for Reinforced Concrete Structures." *Earthquakes and Structures* 2014; **6**: 581-609.

[22] LlanesT, Mario D, Alfredo R, Eden B, Juan B, Arturo Lopez-Barraza, J. Luz Rivera-Salas, and Jose R. GC. Local, Story, and Global Ductility Evaluation for Complex 2D Steel Buildings: Pushover and Dynamic Analysis." *Applied Sciences* 2019**;9**, (1): 200.

List of Symbol

Symbol	Title
R	The distance between source of explosion and structure
W	Mass of blast charge .
Z	Stand-off distance.
f_c'	Compressive strength of unconfined concrete.
ε_c'	Concrete strain at f_c' .
ε_u	Ultimate strain of concrete
ε_y	Yield strain of reinforcing steel.
E_s	Steel modulus of elasticity
f_y	Yield stress of steel
f_u	ultimate stress capacity of steel
ε_{sh}	Strain in steel at the onset of strain hardening
ε_u	Steel ultimate strain capacity
E_c	Modulus of elasticity of concrete
I_g	Moment of initial
A_w	Section area of element
p_k	Nodal forces or stress resultants.
d_{up}	Plastic incremental nodal displacement.
λ	Flow constant
g	Gradient vector of the yield surface
d_p	Plastic deformation of a particular cross-section
k_e	Elastic stiffness matrix of the element.
P.H.	Plastic Hinge
μ	Ductility index
U_{max}	Maximum displacement
U_{yield}	Yield displacement at formation of first plastic hinge
DI	Damage Index
E_p	Potential energy
E_h	Hysteresis energy
$U_{residual}$	Residual displacement
U_{max}	Maximum displacement
$(C.M\text{-}C.S)_X$	The difference between centers of mass and stiffness in X-direction (absolute value)
$(C.M\text{-}C.S)_Y$	The difference between centers of mass and stiffness in Y-direction (absolute value)
m_u	Ultimate moment
p_u	Ultimate axial force